

RSC Advances



This is an *Accepted Manuscript*, which has been through the Royal Society of Chemistry peer review process and has been accepted for publication.

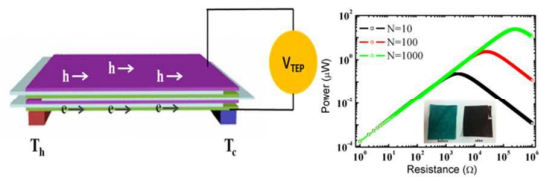
Accepted Manuscripts are published online shortly after acceptance, before technical editing, formatting and proof reading. Using this free service, authors can make their results available to the community, in citable form, before we publish the edited article. This *Accepted Manuscript* will be replaced by the edited, formatted and paginated article as soon as this is available.

You can find more information about *Accepted Manuscripts* in the [Information for Authors](#).

Please note that technical editing may introduce minor changes to the text and/or graphics, which may alter content. The journal's standard [Terms & Conditions](#) and the [Ethical guidelines](#) still apply. In no event shall the Royal Society of Chemistry be held responsible for any errors or omissions in this *Accepted Manuscript* or any consequences arising from the use of any information it contains.

Table of contents entry (TOCE)

Thermoelectric modules were fabricated made of p-type and n-type SWCNT composite papers, demonstrating as efficient thermoelectric materials.





Journal Name

ARTICLE

Evaluation of power generated by thermoelectric modules comprising p-type and n-type single walled carbon nanotube composite paper

Received 00th January 20xx,
Accepted 00th January 20xx

DOI: 10.1039/x0xx00000x

www.rsc.org/

Mingxing Piao[#], Min-Kyu Joo[#], Jun Hee Choi, Jong Mok Shin, Young Sun Moon, Gyu Tae Kim*, Urszula Dettlaff-Weglikowska*

We report on the p-type and n-type thermoelectric (TE) materials made of single-walled carbon nanotube (SWCNT) networks incorporated into the cellulose fiber structure of a common packaging paper. This leads the paper to possess both the mechanical flexibility of cellulose fibers as a supporting matrix and the high electrical conductivity originating from SWCNTs. Thermoelectric power of up to $\pm 50 \mu\text{V/K}$ was successfully obtained as well, depending on their electronic type. Further, to demonstrate its thermoelectric voltage (V_{TEP}) and generating power, a couple of thermoelectric modules composed of both p-type and n-type composite layers were assembled in series. The produced V_{TEP} shows a quasi-linearity with respect to the number of p-n couples and the temperature difference ΔT . Our testing module enables the provision of V_{TEP} and power generation as large as $\approx 16.8 \text{ mV}$ and $\approx 75.5 \text{ nW}$ upon inducing a 50 K temperature difference. The feasibility of commercial TE modules consisting of 10, 100 and 1000 p-n SWCNT couples was numerically calculated, taking into account our experimental results.

1. Introduction

With the excessive consumption of the traditional energy, new eco-efficient, renewable and sustainable energy technologies have recently gained much attention.¹ Thermoelectric (TE) generators have been considered as a candidate for energy-harvesting technologies, converting heat into electricity. They offer a number of advantages: they are compact, have no moving parts, work silently and have low maintenance costs.^{2,3} Low band gap inorganic semiconductors such as Bi_2Te_3 , Sb_2Te_3 and PbTe have been widely employed as TE materials^{4,5} even though they are well known to be toxic, brittle, and expensive for mass production. These disadvantages limit significantly their practical applications in future technologies.

Carbon nanotube (CNT) networks, due to their extraordinary electrical and mechanical properties, are considered for a variety of applications ranging from transparent conductive layers, sensors, conductive fillers for batteries to tissue engineering. To this end, several factors which affect their

performance have been investigated on flexible, rigid and porous substrates.⁶ Furthermore, it has been shown that single walled carbon nanotube (SWCNT) fibers made of SWCNT polyelectrolyte dispersions exhibit ultrahigh electrical conductivity after chemical doping.^{7,8} Also, high performance of multifunctional CNT fibers produced with a simple high throughput wet spinning method has been reported.⁹ More recently, CNT/polymer composites were suggested to replace semiconductor-based TE materials.^{2,10-14} They can offer better mechanical flexibility, light weight as well as low fabrication costs. In particular, SWCNT/polycarbonate composites with a quite high positive Seebeck coefficient ($\approx 65 \mu\text{V/K}$) demonstrated strong capability to convert heat into electricity.¹⁵ However, embedded SWCNTs lose some of their excellent intrinsic electrical conductivity, which is required for efficient TE performance, mainly owing to the insulating properties of polymers. But CNTs forming entangled mats or membranes (bucky papers) still have the potential to demonstrate a sufficient electrical conductivity and a moderate Seebeck coefficient ($\approx 40 \mu\text{V/K}$) that can be exploited in future TE generators.¹⁶

In this paper, we utilize the electrically percolating SWCNT networks to interpenetrate the cellulose fibers of a common paper (instead of bucky papers) to reduce the necessary amount of nanotubes.¹⁷ The prepared composite papers serve as the p-type and n-type TE layers in the assembled TE modules. The following sections give details of the preparation

School of Electrical Engineering, Korea University, 136-701, Seoul, South Korea. E-mail: gtkim@korea.ac.kr, udetlaff.w@gmail.com

[#] these authors contributed equally.

of SWCNT composites, their TE characterization, the assembly of TE modules composed of up to five p-n couples, and performance evaluations of the prepared TE devices. The power generated by the up-scaled TE generators was analyzed for an increasing number of junctions up to 1000 p-n units, and as a function of the applied load resistance.

2. Experimental

The SWCNTs used in this study were synthesized by the chemical vapor deposition method and purchased from Thomas Swan & Co. Ltd, Crockhall, Consett, UK (product reference: PR0920), in the form of a 'wet cake' (containing \approx 5.36 wt.% of SWCNT powder) which improved SWCNT dispersibility in water-based solutions. According to our investigations based on the absorption spectrum, the purchased sample was a heterogeneous mixture of metallic and semiconducting SWCNTs. We estimated the content of semiconducting SWCNTs to be about 60 % in a thin self-supporting film using our experimentally determined relationship between the Seebeck coefficient and the ratio of precisely adjusted pure semiconducting SWCNT to pure metallic SWCNT networks.¹⁸ The diameter of SWCNTs was in the range of 1 - 2 nm, and the nominal length was in the range of $> 1 \mu\text{m}$.

To prepare the SWCNT embedded paper samples, the nanotubes (\approx 100 mg) were dispersed in a 0.5 wt.% solution (100 ml) of sodium dodecylbenzenesulfonate (SDBS, purchased from Aldrich), using a probe sonicator for 20 min. A thin (17 μm), flexible and commercially available colored giftwrap paper was used as SWCNT support due to its outstanding tear resistance and its absorptivity. The well dispersed SWCNT solution was introduced dropwise onto the paper until it was saturated with liquid. It was observed that the SWCNT solution was easily absorbed by the fiber structure of the paper, due to capillary forces. After being completely dried in an oven at 80°C, the paper was then immersed into deionized water for 20 min to remove SDBS. This entire process was carried out six times until the paper was sufficiently soaked with nanotubes, identified by its change in color from green to black and its improved electrical conductivity. The untreated paper was an electrical insulator. Pristine as-prepared SWCNTs are commonly p-doped through ambient oxygen. Incorporated into cellulose fibers of paper, they serve as a p-type TE material. A chemical post-treatment of the composite paper with polyethyleneimine (PEI) changes the doping of SWCNTs from p-type to n-type, producing an n-type TE material. To this end, the prepared SWCNT composite papers were immersed in a water solution (0.6 wt.%) of PEI (capped with amine groups at the end of polymer chain, average molecular weight of 600, purchased from Aldrich) for 15 min and then dried in air for 30 min. Both p-type and n-type SWCNT composite papers were completely black, electrically conductive and flexible, with an unchanged thickness of 17 μm . The papers were cut into strips (10 \times 30 mm), combined into p-n couples and assembled into TE modules. The electrical contact at the ends of the strips was achieved by mechanical

compressing of the ends of the sample strips. Compact TE modules were arranged as an alternating assembly of p-n SWCNT composite papers, with polyethylene terephthalate (PET) acting as an insulating layer between them.

The measurement of the electrical resistance of the prepared samples was performed using the standard four probe method at room temperature, applying the electrical current (Keithley 238) and measuring the voltage (34401A multimeter, Hewlett-Packard). The measured resistance was converted into electrical conductivity by multiplying it by the geometric factor of the sample. To determine the Seebeck coefficient, the thermoelectric voltage (V_{TEP}) induced along the paper sample by temperature difference ($\Delta T = T_{\text{h}} - T_{\text{c}}$, where T_{h} and T_{c} were the temperatures of the hot and cold side, respectively) was measured simultaneously. The detailed method for the Seebeck coefficient measurement along with the performance determination of the fabricated TE modules has been described elsewhere.¹⁵

3. Results and discussion

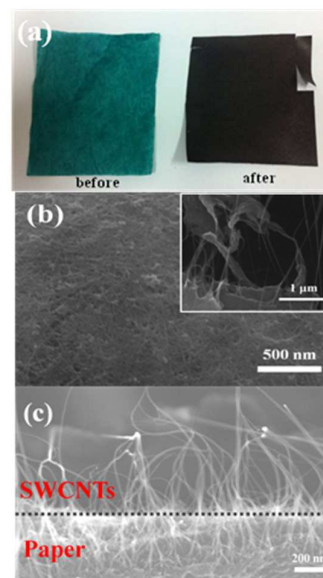


Fig. 1 (a) Optical images of a commercial packaging paper before (left) and after (right) absorption of the SWCNT dispersion. Representative FESEM images of (b) the paper surface covered with a dense copacted SWCNT network (Inset: cellulose fibers and stretched nanotube bundles bridging the paper pore), (c) the cross-sectional image of the SWCNT/paper composite, respectively.

Fig. 1a displays two photographs of the paper used for our experiment, taken before and after introduction of SWCNTs. The composite paper was completely black, electrically conductive, tear-proof and flexible, with a thickness of 17 μm . Observations of the surface and cross-section of the SWCNT/paper composite *via* a field emission scanning electron microscope (FESEM) revealed long, numerous and uniform

SWCNT bundles homogenously dispersed on the paper surface as well as interpenetrating the porous paper structure, as presented in Fig. 1b and 1c. Furthermore, stretched nanotube bundles bridging the paper pore were visible besides some cellulose fibers (inset of Fig. 1b). As a result, the formation of percolated conducting paths on the surface, partially penetrating the volume of the supporting matrix has been achieved. The paper soaked with SWCNTs provides a composite material, where mechanical flexibility of cellulose fibers is combined with high electrical conductivity of SWCNTs. While pristine SWCNTs incorporated between cellulose fibers of paper deliver a p-type TE material due to commonly p-type doping of SWCNTs under ambient conditions, a chemical post-treatment of the composite paper with PEI changes the doping of SWCNTs from p-type to n-type, producing an n-type TE material. PEI as an amine-rich polymer is often applied as an effective n-type dopant for SWCNTs.¹⁹ The composite papers were characterized as possible materials for TE power generation.

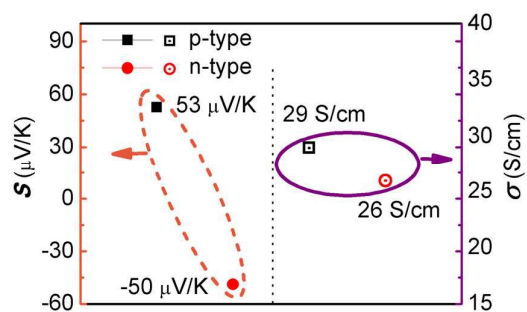


Fig. 2 The Seebeck coefficient (S) and electrical conductivity (σ) of the p-type and n-type SWCNT composite papers.

The electrical conductivity and the Seebeck coefficient of both p-type and n-type SWCNT composite papers are shown in Fig. 2. The electrical conductivity of the p-type and n-type SWCNT papers was found to be almost equal and independent of the available majority charge carriers at ≈ 29 S/cm and ≈ 26 S/cm, respectively. This result demonstrates that the doping with PEI did not greatly affect the charge mobility and the electrical conductivity of SWCNTs in the composite paper. The value of electrical conductivity is comparable or even higher than that measured for pure self-supporting CNT films (bucky papers).²⁰⁻²³ Similarly, the absolute values of the Seebeck coefficient were almost identical for the p-type and n-type SWCNT papers with $+53$ $\mu\text{V/K}$ and -50 $\mu\text{V/K}$, respectively. The Seebeck coefficient of the p-type paper was slightly higher than that of SWCNT bucky paper ($+40$ $\mu\text{V/K}$), indicating that the cellulose fibers of the paper filtered the low energy carriers through increasing the phonon scattering in the composite.²⁴ The Seebeck coefficient of the n-type SWCNT papers (-50 $\mu\text{V/K}$) indicates clearly that the majority of charge carriers in p-type SWCNT networks were completely converted from holes to electrons by the efficient adsorption of PEI molecules on the surface of the SWCNTs.²⁵ Accordingly to the

TE properties of the p-type and n-type composite papers, the power factor $P=S^2\sigma$, commonly used as a measure of TE efficiency, was also compared (≈ 8.15 $\mu\text{W/mK}^2$ for p-type and ≈ 6.5 $\mu\text{W/mK}^2$ for the n-type papers, respectively).

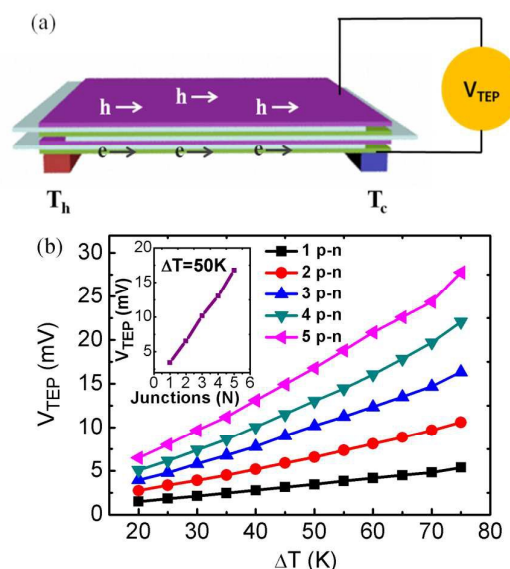


Fig. 3 (a) Schematic of the TE module involving two couples composed of p-type (violet) and n-type (green) SWCNT composite papers and insulating films of PET (blue) exposed to the temperature gradient $\Delta T = T_h - T_c$, the flow of the charge carriers is indicated by the arrows, (b) The measured V_{TEP} as a function of ΔT for a series of TE modules with up to five p-n couples, the inset shows the linear dependence of V_{TEP} on the number of p-n couples in the assembled modules when $\Delta T = 50$ K.

In order to generate a sufficient power output, p-type and n-type TE materials are usually combined into TE modules.²⁶⁻²⁹ Here, the p-type and n-type composite papers were assembled in modules with alternative p-n couples electrically connected in series (compressed ends of paper strips) and thermally in parallel, as shown in Fig. 3a. The induced V_{TEP} as a function of ΔT with respect to the number of p-n couples in the module was measured and displayed in Fig. 3b. It clearly demonstrates the Seebeck effect, *i.e.*, the measured V_{TEP} increases almost linearly with the gradual change of ΔT . Moreover, the linear dependence of V_{TEP} on the number of p-n couples in the module at $\Delta T = 50$ K is visible in the inset of Fig. 3b. This property is meaningful for the fabrication of commercial TE modules consisting of hundreds of p-n couples.

For a module testing, a set of ΔT values was induced across it and V_{TEP} and current were measured simultaneously to calculate the power generation. To optimize the maximum power generation, the voltage and current from TE modules composed of one, three and five p-n couples were measured at $\Delta T = 50$ K as a function of different load resistance values (R_L). The generated power is illustrated in Fig. 4a. The achieved maximal power (when the load resistance matched the corresponding internal module resistance), was ≈ 14.7 , ≈ 54.5

and ≈ 75.5 nW for one, three and five p-n couples, respectively. The maximal power output and the internal module resistance as a function of the number of p-n couples N are shown in the inset of Fig. 4a. It might be naturally accepted that both the V_{TEP} and the maximal power output could be significantly improved by increasing N , while the internal module resistance was simply the sum of the unit resistances of N involved p-n couples. The development of V_{TEP} produced by five p-n couples for several different load resistances upon application $\Delta T = 50$ K is shown in Fig. 4b. At the load resistance related to the maximum power generation, the $V_{\text{TEP}} \approx 7.8$ mV compared to an open circuit $V_{\text{TEP}} \approx 16.8$ mV at the same ΔT . Above this resistance, the V_{TEP} continuously increased with the load resistance approaching the open circuit voltage, whereas the power output dramatically decreased with an exponentially increasing load resistance. The power output versus ΔT at a load resistance of 850Ω is shown in the inset of Fig. 4b and demonstrates a squared behavior of the generated power as a function of ΔT as a result of the relationship V_{TEP}^2/R_L . Thus, the maximum power ≈ 75.5 nW generated by TE module exposed to a $\Delta T = 50$ K could be improved up to ≈ 180 nW by enhancing ΔT up to 70 K.

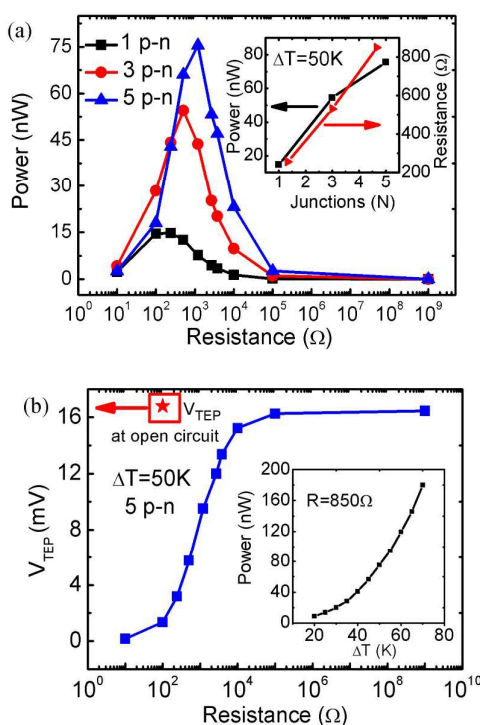


Fig. 4 (a) The generated power as a function of load resistance for modules with one, three and five p-n couples at $\Delta T = 50$ K, the inset shows the maximal power and the internal resistance of the TE device as a function of the junction number N in the module, (b) V_{TEP} produced by five p-n couples at open circuit and under loading with resistance at $\Delta T = 50$ K, the inset shows the power output as a function of ΔT for a load resistance of 850Ω .

Taking into account the fact that commercial TE modules consist of hundreds of p-n couples, we calculated the feasible power generated when $N = 10, 100$, and 1000 p-n couples as a function of load resistance keeping $\Delta T = 50$ K. The results are presented in Fig. 5a. As expected, the increase in N dramatically improved the module power. Here, a module of $N = 10$ p-n units generated ≈ 232 nW for load resistance of 2.6 k Ω , while the maximum power of a module containing 1000 units was as high as $\approx 23 \mu\text{W}$. However, the corresponding load resistance also increased up to ≈ 290 k Ω . We also investigated the power output with an increasing number N of p-n couples while taking into account three different load resistances ($R_L = 1.2, 10$ and 100 k Ω), as illustrated in Fig. 5b. At first the generated power increased rapidly with increasing N , and then reached saturation even though the number of p-n couples continued to increase. The number of p-n couples required for maximal power was increased depending on the load resistance. For example, at a load resistance of 1.2 k Ω , the generated power reached saturation when the module comprised 16 p-n couples. This number increased to 550 when the load resistance was increased to 100 k Ω . Hence, depending on the applied load resistance, an appropriate TE module composed of a required number of p-n couples can be fabricated for an optimal use of the generated power.

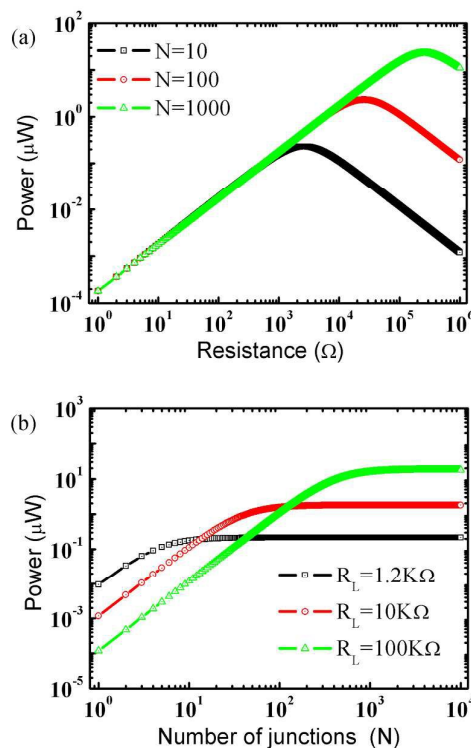


Fig. 5 (a) Theoretical power output calculated for modules with 10, 100 and 1000 p-n couples under different load resistances and exposed to $\Delta T = 50$ K, (b) The numerically simulated results of generated power as a function of the number of p-n couples in a module when loaded with three different resistance values.

4. Conclusions

Both p-type and n-type SWCNT composite papers were prepared. The electrical conductivity and the Seebeck coefficient were determined in order to use the papers as TE materials. To this end, several TE modules were fabricated by combining p-type and n-type SWCNT composite papers into electrically conductive junctions. Their TE performances, including V_{TEP} and generated power, were investigated as a function of the number of p-n couples, temperature difference ΔT and load resistance R_L . It was demonstrated that a TE module composed of five p-n couples produced V_{TEP} as high as ≈ 16.8 mV when exposed to $\Delta T = 50$ K and generated ≈ 75.5 nW of power when the load resistance $R_L \approx 850 \Omega$. The power output could be improved by increasing the number of p-n couples and the applied temperature difference ΔT . The theoretical estimated power output could be as high as $\approx 23 \mu W$ for 1000 p-n couples. Our results open up new possibilities to fabricate flexible, low cost, organic TE devices involving the extraordinary electrical and thermal transport properties of SWCNT networks incorporated in the structure of cellulose fibers of common paper.

Acknowledgements

This work was supported by BK21 Plus Humanware Information Technology, the Center for Advanced Soft Electronics under the Global Frontier Research Program of the Ministry of Education (NRF-2014M3A6A5060942).

References

- 1 K. Yazawa and A. Shakouri, *Environ. Sci. Technol.*, 2011, **45**, 7548.
- 2 C. Z. Meng, C. Liu and S. Fan, *Adv. Mater.*, 2010, **22**, 535.
- 3 M. S. Dresselhaus, G. Chen, M. Y. Tang, R. G. Yang, H. Lee, D. Z. Wang, Z. F. Ren, J. P. Fleurial and P. Gogna, *Adv. Mater.*, 2007, **19**, 1043.
- 4 Y. Choi, Y. Kim, S. G. Park, Y. G. Kim, B. J. Sung, S. Y. Jang and W. Kim, *Org. Electron.*, 2011, **12**, 2120.
- 5 O. Bubnova, Z. U. Khan, A. Malti, S. Braun, M. Fahlman, M. Berggren and X. Crispin, *Nat. Mater.*, 2011, **10**, 429.
- 6 A. Saha, C. Jiang and A. A. Marti', *Carbon*, 2014, **79**, 1.
- 7 C. Jiang, A. Saha, C. Xiang, C. C. Young, J. M. Tour, M. Pasquali and A. A. Marti', *ACS Nano*, 2013, **7**, 4503.
- 8 C. Jiang, A. Saha, C. C. Young, D. P. Hashim, C. E. Ramirez, P. M. Ajayana, M. Pasquali and A. A. Marti', *ACS Nano*, 2014, **8**, 9107.
- 9 N. Behabtu, C. C. Young, D. E. Tsentelovich, O. Kleinerman, X. Wang, A. W. K. Ma, E. A. Bengio, R. F. ter Waarbeek, J. J. de Jong, R. E. Hoogerwerf, S. B. Fairchild, J. B. Ferguson, B. Maruyama, J. Kono, Y. Talmon, Y. Cohen, M. J. Otto and M. Pasquali, *Science*, 2013, **339**, 182.
- 10 C. A. Hewitt, A. B. Kaiser, S. Roth, M. Craps, R. Czerw and D. L. Carroll, *Appl. Phys. Lett.*, 2011, **98**, 183110.
- 11 C. Yu, K. Choi, L. Yin and J. C. Grunlan, *ACS Nano*, 2011, **5**, 7885.
- 12 D. D. Freeman, K. Choi and C. Yu, *Plos One*, 2012, **7**, e47822.
- 13 Q. Yao, L. Chen, W. Zhang, S. C. Liufu and X. Chen, *ACS Nano*, 2010, **4**, 2445.
- 14 C. Yu, Y. S. Kim, D. Kim and J. C. Grunlan, *Nano Lett.*, 2008, **8**, 4428.
- 15 M. X. Piao, G. T. Kim, G. P. Kennedy, S. Roth and U. Dettlaff-Weglikowska, *Phys. Status Solidi B*, 2013, **250**, 1468.
- 16 M. X. Piao, M. R. Alam, G. T. Kim, U. Dettlaff-Weglikowska and S. Roth, *Phys. Status Solidi B*, 2012, **249**, 2353.
- 17 T. Tanaka, E. Sano, M. Imai and K. J. Akiyama, *Appl. Phys.*, 2010, **107**, 054307.
- 18 M. Piao, M. Joo, J. Na, Y. Kim, M. Mouis, G. Ghibaudo, S. Roth, W. Kim, H. Jang, G. P. Kennedy, U. Dettlaff-Weglikowska and G. Kim, *J Phys. Chem. C*, 2014, **118**, 26454.
- 19 Y. Ryu, D. Freeman and C. Yu, *Carbon*, 2011, **49**, 4745.
- 20 G. Trakakis, D. Tasis, J. Parthenios, C. Galiotis and K. Papagelis, *Materials*, 2013, **6**, 2360.
- 21 Y. Xing, X. Zhang, H. Chen, M. Chen and Q. Li, *Carbon*, 2013, **61**, 501.
- 22 J. Zhang, D. Jiang, H. Peng and F. Qin, *Carbon*, 2013, **63**, 125.
- 23 S. Sakurai, F. Kamada, D. N. Futaba, M. Yumura and K. Hata, *Nanoscale Res. Lett.*, 2013, **8**, 546.
- 24 A. B. Kaiser, *Phys. Rev. B*, 1989, **40**, 2806.
- 25 Y. M. Choi, D. S. Lee, R. Czerw, P. W. Chiu, N. Grobert, M. Terrones, M. Reyes-Reyes, H. Terrones, J. C. Charlier, P. M. Ajayan, S. Roth, D. L. Carroll and Y. M. Park, *Nano Lett.*, 2003, **3**, 839.
- 26 C. Hu, C. Liu, L. Chen, C. Meng and S. Fan, *ACS Nano*, 2010, **4**, 4701.
- 27 C. A. Hewitt, A. B. Kaiser, S. Roth, M. Craps, R. Czerw and D. L. Carroll, *Nano Lett.*, 2012, **12**, 1307.
- 28 C. Yu, A. Murali, K. Choi and Y. Ryu, *Energy Environ. Sci.*, 2012, **5**, 9481.
- 29 M. Piao, J. Na, J. Choi, J. Kim, G. P. Kennedy, G. Kim, S. Roth, and U. Dettlaff-Weglikowska, *Carbon*, 2013, **62**, 430.